Anal Bioanal Chem (2007) 387:2121–2130
DOI 10.1007/s00216-006-1088-8

ORIGINAL PAPER

Cation identity dependence of crown ether photonic crystal Pb^{2+} sensing

Fangyong Yan · Sanford Asher

Received: 22 September 2006 / Revised: 6 December 2006 / Accepted: 8 December 2006 / Published online: 16 February 2007

Abstract We quantitatively modeled the volume phase transition of a hydrogel containing a crystalline colloidal array with a crown ether ligand which binds Pb^{2+}. The hydrogel volume response and the wavelength diffracted depend on the Pb^{2+} concentration and on both the ionic strength and the valence of the nonbinding ionic species. We successfully modeled the response of this hydrogel Pb^{2+} sensor to ionic strength and the cation valence of the added salts.

Keywords Phase transition · Hydrogel · Crystalline colloidal array · Crown ether ligand · Ionic strength · Wavelength diffracted

Introduction

Hydrogels are crosslinked polymers containing water [1–9]. Hydrogels in equilibrium with aqueous solutions adopt a defined volume such that there is a balance between the osmotic pressure associated with the free energy of mixing of the hydrogel polymer with the solution, the osmotic pressure associated with ionic interactions due to bound charges and counterions, and the osmotic pressure associated with the elastic restoring force due to the polymer chain entropy [1]. Modest changes in the solution chemical composition can dramatically change the hydrogel volume because these changes cause significant changes in the osmotic pressure [1–5, 10–16].

F. Yan · S. Asher (✉)
Department of Chemistry, Chevron Science Center,
University of Pittsburgh,
Pittsburgh, PA 15260, USA
e-mail: asher@pitt.edu

The resulting hydrogel volume changes, which have been labeled hydrogel volume phase transitions, are of fundamental interest. In addition, these phenomena are useful when fabricating smart materials [2–5, 17–19]. For example, these volume phase transitions are used in drug delivery, where the hydrogel volume is chemically controlled in order to increase the diffusion of drugs out of the hydrogel [5–9, 18–21].

We have utilized these hydrogel volume phase transitions for chemical sensing purposes. We incorporated crystalline colloidal arrays (CCAs) into hydrogels, forming polymerized crystalline colloidal arrays (PCCAs). These PCCAs effectively diffract visible wavelength light. Hydrogel volume changes shift the diffracted wavelength of the CCA. This enables us to sensitively monitor the hydrogel volume [22–32]. We attach molecular recognition agents which actuate hydrogel volume changes. We have utilized recognition agents which change the hydrogel pH, in order to titrate hydrogel pendant groups which change the overall hydrogel free energy of mixing [30–32]. We also developed recognition motifs where crosslinks are formed to shrink the hydrogel in order to blue-shift the diffraction [29]. We also developed motifs where charged analytes chelate such that the hydrogel becomes charged and the diffraction redshifts [22–28].

In this case, a Donnan potential forms, giving rise to a very large hydrogel volume response in low ionic strength solutions at very low analyte concentrations for analytes with large association constants. The response in this case shows a large dependence on solution ionic strength. We have previously successfully modeled the response of sensing hydrogels containing crown ether groups with a large binding constant for Pb^{2+} [27]. In the work described here, we extend this modeling to more complex situations where the solutions contain pure or mixed salts with a variety of valencies.

Experimental

Materials NaCl (JT Baker), $NaNO_3$ (JT Baker, Phillipsburg, NJ, USA), $Mg(NO_3)_2$ (JT Baker), $Al(NO_3)_3$ (JT Baker), $Pb(NO_3)_2$ (MCB, South Plainfield, NJ, USA) were used as received. 18 MΩ purified water was obtained from a NANOpure Infinity purification system (Barnstead/Thermolyne Corp., Dubuque, IA, USA). Highly charged, monodisperse polystyrene colloids were prepared via emulsion polymerization [33].

PCCA preparation We fabricated the PCCA Pb^{2+} sensor using methods described previously [22–24, 27]. We polymerized a solution containing 160 mg of acrylamide (Fluka, Buchs, Switzerland), 13.2 mg *N*,*N*′-methylenebis-acrylamide (Fluka), 36.0 mg 4-acrylamidobenzo-18-crown-6 (dissolved in DMSO, Acros Organics, Geel, Belgium), and 3.2 ml of a 4.9% dispersion of 90-nm-diameter highly charged, monodisperse polystyrene colloidal particles [33]. The resulting dispersion diffracted 490 nm light incident normal to the fcc 111 planes oriented parallel to the container walls. Wet ion exchange resin (Bio-Rad, Hercules, CA, USA; mixed bed AG501-X8(D)) and two drops of concentrated diethoxyacephenone (Aldrich, St. Louis, MO, USA) were added and the mixture was shaken for 30 min. The mixture was centrifuged to eliminate air bubbles and injected into a cell consisting of two quartz plates separated by a parafilm spacer (125 μm thick). The colloidal particles self-assembled into a CCA to give a diffracting liquid film (diffraction maximum 500 nm for normal incident light). The film was photopolymerized into a PCCA by exposure for five hours to 365 nm UV light from two mercury lamps (Black Ray, UV Products Inc., San Gabriel, CA, USA). The polymerizing cell was opened, and the PCCA was washed overnight with DI water.

Measurements Diffraction spectra were measured using a USB2000 Fiber Optic Spectrometer and a LS-1 Tungsten Halogen Light Source (Ocean Optics Inc., Dunedin, FL, USA). The PCCA's response to Pb^{2+} was measured either with the PCCA attached to a quartz plate (1-D swelling), or with the PCCA film free (3-D swelling).

Results and discussion

Determination of Flory–Huggins parameter and the effective crosslink density The PCCA is a hydrogel which consists of a crosslinked polymeric network in water [22–32]. According to Flory theory, the evolution to the equilibrium volume of a hydrogel is governed by three free energy differences between the existing volume and the equilibrium volume: the mixing free energy between the polymer chains and the solvent molecules (ΔG_M), the ionic free energy of the polymer solution (ΔG_{ion}), and the elastic free energy of the polymer gel network (ΔG_{el}). At equilibrium, the net osmotic pressure due to the three free energies is zero [1]:

$$\Pi_{net} = \frac{\partial \Delta G}{\partial V} = \Pi_M + \Pi_{ion} + \Pi_{el} = 0 \tag{1}$$

where Π_{net} is the net osmotic pressure, Π_M is the osmotic pressure due to the mixing of polymer chains with the solvent molecules, Π_{ion} is the osmotic pressure due to the ionic free energy of the polymer solution, and Π_{el} is the osmotic pressure due to the elastic free energy of the polymer network.

Π_M has been derived by Flory [1] as:

$$\Pi_M = -\frac{RT}{\overline{V_s}}\left[\ln\left(1-\frac{V_0}{V}\right)+\frac{V_0}{V}+\chi\left(\frac{V_0}{V}\right)^2\right] \tag{2}$$

where R is the universal gas constant, T is the temperature in the gel, $\overline{V_s}$ is the molar volume of solvent in the gel, χ is the Flory–Huggins parameter, V_0 is the volume of the dry hydrogel, and V is the equilibrium volume of the hydrogel.

There are two models for Π_{el}, the affine model and the phantom model, which represent the two extreme conditions for deformation of the hydrogel network. The fundamental difference between these two models is that the crosslink junctions are considered fixed in the affine model, but are allowed to vary from their mean positions in the phantom model [1, 34–39]. In the 3-D swelling model, the hydrogel swells isotropically in three dimensions and Π_{el} is

$$\begin{aligned}\Pi_{el} &= -RTv_e\left[\left(\frac{V}{V_m}\right)^{\frac{1}{3}}-\frac{1}{2}\left(\frac{V_m}{V}\right)\right] && \text{affine model}\\ &= -\frac{RTv_e}{2}\left(\frac{V_m}{V}\right)^{\frac{1}{3}} && \text{phantom model}\end{aligned} \tag{3}$$

where v_e is the effective crosslink density in the network and V_m is the volume of gel prepared (before washing).

In the 1-D swelling model, the hydrogel can only swell along one dimension, and Π_{el} is:

$$\begin{aligned}\Pi_{el} &= -RTv_e\left[\left(\frac{V_m}{V}\right)-\frac{1}{2}\left(\frac{V_m}{V}\right)\right] && \text{affine model}\\ &= -\frac{RTv_e}{2}\left(\frac{V}{V_m}\right) && \text{phantom model}\end{aligned} \tag{4}$$

The PCCA hydrogel diffracts light from the fcc 111 planes of the embedded CCA. These planes are parallel to the film surface and diffract according to Bragg's law [33, 40–45]:

$$m\lambda = 2nd\sin(\theta) \tag{5}$$

where m is the diffraction order. The diffracted wavelength λ depends on the 111 plane spacing d, and the refractive index of the system n. θ is the Bragg glancing angle.

We measure the first order diffracted wavelength using $m=1$, and θ is kept constant at 90°. Thus, $\lambda \propto d$, since n is relatively constant. Based on Eq. 5, the relationship between the volume and the diffracted wavelength of the PCCA is

$$\frac{V_m}{V} = \frac{(\lambda_m)^j}{\lambda^j}$$
$$\frac{V_0}{V} = \frac{(\lambda_0)^j}{\lambda^j} \quad (6)$$

where λ_m, λ_0 and λ are the diffracted wavelengths for the prepared PCCA, the dry PCCA and the PCCA in the volume equilibrium. j is a dimensional coefficient. For the 1-D swelling model $j=1$, and for the 3-D swelling model $j=3$.

For a nonionic hydrogel, Π_{ion} is zero and at equilibrium:

$$\Pi_{net} = \Pi_M + \Pi_{el} = 0 \quad (7)$$

Substituting Eqs. 2, 3, 4 and 6 into 7 leads to the volume equilibrium condition of the PCCA in pure water in the affine and phantom models:

$$v_e\left[\left(\frac{\lambda}{\lambda_m}\right) - \frac{1}{2}\left(\frac{\lambda_m}{\lambda}\right)\right] + \frac{1}{\overline{V_s}}\left[\ln\left(1-\frac{\lambda_0}{\lambda}\right) + \frac{\lambda_0}{\lambda} + \chi\left(\frac{\lambda_0}{\lambda}\right)^2\right] = 0 \quad (8a)$$

$$v_e\left[\left(\frac{\lambda_m}{\lambda}\right) - \frac{1}{2}\left(\frac{\lambda_m}{\lambda}\right)^3\right] + \frac{1}{\overline{V_s}}\left[\ln\left(1-\left(\frac{\lambda_0}{\lambda}\right)^3\right) + \left(\frac{\lambda_0}{\lambda}\right)^3 + \chi\left(\frac{\lambda_0}{\lambda}\right)^6\right] = 0 \quad (8b)$$

$$\frac{v_e}{2}\left(\frac{\lambda}{\lambda_m}\right) + \frac{1}{\overline{V_s}}\left[\ln\left(1-\frac{\lambda_0}{\lambda}\right) + \frac{\lambda_0}{\lambda} + \chi\left(\frac{\lambda_0}{\lambda}\right)^2\right] = 0 \quad (9a)$$

$$\frac{v_e}{2}\left(\frac{\lambda_m}{\lambda}\right) + \frac{1}{\overline{V_s}}\left[\ln\left(1-\left(\frac{\lambda_0}{\lambda}\right)^3\right) + \left(\frac{\lambda_0}{\lambda}\right)^3 + \chi\left(\frac{\lambda_0}{\lambda}\right)^6\right] = 0 \quad (9b)$$

where Eqs. 8a, 8b are for the 1-D and 3-D affine models, and Eqs. 9a and 9b are for the 1-D and 3-D phantom models.

In our PCCA sensor, λ_m was measured to be 500 nm, λ was 642 nm for the hydrogel attached to a substrate which allows only 1-D swelling. λ was 576 nm for a free PCCA which could swell in 3-D. Based on Eq. 6, λ_0 was calculated to be 19 nm in the 1-D swelling model and 169 nm in the 3-D swelling model. Combining Eqs. 8a and 8b, we calculate that in the affine model, $\nu_e = 6.80\times10^{-4}$ M (only 2.5% of the *N*,*N*′-methylenebisacrylamide forms effective crosslinks) and $\chi = 0.499$.

By combining Eqs. 9a and 9b, we calculate that in the phantom model, $\nu_e = 3.25\times10^{-3}$ M (12% of *N*,*N*′-methylenebisacrylamide forms effective crosslinks) and $\chi = 0.47$. These values of χ are close to those previously determined for similar PCCAs (where χ was 0.503 for the affine model and 0.495 (or 0.493) for the phantom model) [27, 30]. We choose to use the affine model because it calculates a χ value closer to the value of χ previously determined compared to the phantom model.

Modeling the response of PCCA to $Pb(NO_3)_2$ in DI water The PCCA crown ether binds Pb^{2+} selectively. The binding of Pb^{2+} results in the immobilization of its counterion, which results in the formation of a Donnan potential. The Donnan potential results in an osmotic pressure, which swells the hydrogel in proportion to the Pb^{2+} concentration [1, 22, 26, 27, 30]. The Donnan osmotic pressure Π_{ion} can be approximated by [1]:

$$\Pi_{ion} = RT\sum_i \left(C_i - C_i^*\right) \quad (10)$$

where C_i and C_i^* are the concentrations of mobile ions inside and outside of the PCCA, respectively.

At equilibrium, the net osmotic pressure inside the hydrogel is zero, and multiple equilibrium conditions are met simultaneously:

1. The activity of $Pb(NO_3)_2$ inside the hydrogel is the same as that outside the hydrogel [1].

$$\left[Pb^{2+}\right]_{in}\left(\left[NO_3^-\right]_{in}\right)^2 = \left[Pb^{2+}\right]_{out}\left(\left[NO_3^-\right]_{out}\right)^2 \quad (11)$$

   where $[Pb^{2+}]_{in}$ and $[Pb^{2+}]_{out}$ are the concentrations of mobile Pb^{2+} inside and outside the hydrogel. $[NO_3^-]_{in}$ and $[NO_3^-]_{out}$ are the concentrations of mobile NO_3^- inside and outside the hydrogel.
2. At equilibrium, there must be electroneutrality within the hydrogel [1]:

$$2\left[\left(PCCA - PbL^{2+}\right)\right] + 2\left[Pb^{2+}\right]_{in} - \left[NO_3^-\right]_{in} = 0 \quad (12)$$

   ($PCCA{-}PbL^{2+}$) is the PCCA crown ether attached to Pb^{2+}

$$\left[\left(PCCA - PbL^{2+}\right)\right] = \frac{n\_L}{V}\frac{K\left[Pb^{2+}\right]_{in}}{1+K\left[Pb^{2+}\right]_{in}} \quad (13)$$

where K is the binding constant of PCCA crown ether, n_L are the number of moles of crown ether in the hydrogel, and

V is the equilibrium volume of the hydrogel.

Combining Eqs. 12 and 13 yields

$$2\left[Pb^{2+}\right]_{in}+\frac{2K\left[Pb^{2+}\right]_{in}}{1+K\left[Pb^{2+}\right]_{in}}\frac{n-L}{V}-\sqrt{\frac{\left[Pb^{2+}\right]_{out}}{\left[Pb^{2+}\right]_{in}}}\left[NO_3^-\right]_{out}=0 \tag{14}$$

It should be noted that the PCCA crown ether concentration changes with the volume of hydrogel.

Combining Eqs. 1–4, 6, 10 and 11 leads to

$$\left[Pb^{2+}\right]_{in}+\sqrt{\frac{\left[Pb^{2+}\right]_{out}}{\left[Pb^{2+}\right]_{in}}}\left[NO_3^-\right]_{out}-\left[Pb^{2+}\right]_{out}-\left[NO_3^-\right]_{out}+\frac{1}{\overline{V_s}}\left[\ln\left(1-\frac{V_0}{V}\right)+\frac{V_0}{V}+\chi\left(\frac{V_0}{V}\right)^2\right]+v_e\left(\frac{V}{V_m}-\frac{1}{2}\frac{V_m}{V}\right)=0 \tag{15a}$$

$$\left[Pb^{2+}\right]_{in}+\sqrt{\frac{\left[Pb^{2+}\right]_{out}}{\left[Pb^{2+}\right]_{in}}}\left[NO_3^-\right]_{out}-\left[Pb^{2+}\right]_{out}-\left[NO_3^-\right]_{out}+\frac{1}{\overline{V_s}}\left[\ln\left(1-\frac{V_0}{V}\right)+\frac{V_0}{V}+\chi\left(\frac{V_0}{V}\right)^2\right]+v_e\left[\left(\frac{V_m}{V}\right)^{\frac{1}{3}}-\frac{1}{2}\frac{V_m}{V}\right]=0 \tag{15b}$$

$$\left[Pb^{2+}\right]_{in}+\sqrt{\frac{\left[Pb^{2+}\right]_{out}}{\left[Pb^{2+}\right]_{in}}}\left[NO_3^-\right]_{out}-\left[Pb^{2+}\right]_{out}-\left[NO_3^-\right]_{out}+\frac{1}{\overline{V_s}}\left[\ln\left(1-\frac{V_0}{V}\right)+\frac{V_0}{V}+\chi\left(\frac{V_0}{V}\right)^2\right]+\frac{v_e}{2}\frac{V}{V_m}=0 \tag{15c}$$

$$\left[Pb^{2+}\right]_{in}+\sqrt{\frac{\left[Pb^{2+}\right]_{out}}{\left[Pb^{2+}\right]_{in}}}\left[NO_3^-\right]_{out}-\left[Pb^{2+}\right]_{out}-\left[NO_3^-\right]_{out}+\frac{1}{\overline{V_s}}\left[\ln\left(1-\frac{V_0}{V}\right)+\frac{V_0}{V}+\chi\left(\frac{V_0}{V}\right)^2\right]+\frac{v_e}{2}\left(\frac{V_m}{V}\right)^{\frac{1}{3}}=0 \tag{15d}$$

where Eqs. 15a, 15b are for the 1-D and 3-D affine models, and Eqs. 15c and 15d are for the 1-D and 3-D phantom models.

Combining Eq. 14 with 15a, 15b, 15c and 15d, we can determine the values of $[Pb^{2+}]_{in}$ and V in these four models. We can then model the volume change ratio V/V_m of PCCA as a function of Pb^{2+} concentration in the four models. This allows us to calculate, using Eq. 7, the relative diffraction wavelength ratio (λ/λ_m) as a function of Pb^{2+} concentration.

Modeling the response of PCCA to $Pb(NO_3)_2$ in multiple-ion solution The increased ionic strength resulting from the addition of electrolytes to the solution results in a decrease in Π_{ion}, which shrinks the PCCA [24, 27, 28, 30]. We modeled the response of the PCCA to $Pb(NO_3)_2$ in the presence of $NaNO_3$, NaCl, $Mg(NO_3)_2$, and $Al(NO_3)_3$. The 18-crown-6 complex shows log K values of 0.8 and 4.27 for Na^+ and Pb^{2+}, respectively [22, 46, 47]. Thus, a 2,000-fold excess of Na^+ is required to compete with Pb^{2+} binding [22]. The binding constant for Mg^{2+} is less than that for Na^+, and higher than Al^{3+} [48, 49]. Thus, we neglect binding of the PCCA crown ether to Na^+, Mg^{2+} and Al^{3+}.

The equilibrium conditions needed for the PCCA for these solutions lead to the following conditions:

$$\left[A^{j+}\right]_{in}\left([B^-]_{in}\right)^j=\left[A^{n+}\right]_{out}\left([B^-]_{out}\right)^j \tag{16a}$$

$$j\left[A^{j+}\right]_{in}+2\left[Pb^{2+}\right]_{in}+2\left[(PCCA-PbL)^{2+}\right]-\left[NO_3^-\right]_{in}-\left[B^-\right]_{in}=0 \tag{16b}$$

where AB represents $NaNO_3$, NaCl, $Mg(NO_3)_2$ or $Al(NO_3)_3$, with A^{j+} as the cation and B^- as the anion. Equation 16a is based on the equality of the activities of AB_n inside and outside the PCCA hydrogel, while 16b is based on the electroneutrality inside the PCCA.

Following the same procedure to model the response of the PCCA to Pb^{2+} in DI water, we can establish the volume change ratio V/V_m of the PCCA as a function of Pb^{2+} concentration in the four models by using Eqs. 16a and 16b.

PCCA response to $Pb(NO_3)_2$ in DI water (1-D swelling model) The diffracted wavelength of the PCCA in DI water was measured to be 642 nm. A series of standard $Pb(NO_3)_2$ solutions were prepared in 100 mL volumetric flasks. We measured the response of the PCCA to $Pb(NO_3)_2$ by exposing the PCCA to these solutions. Between different Pb^{2+} solutions, the PCCA was washed by immersing it in a stirred reservoir of pure water until the diffracted wavelength of the sensor returned to 642 nm.

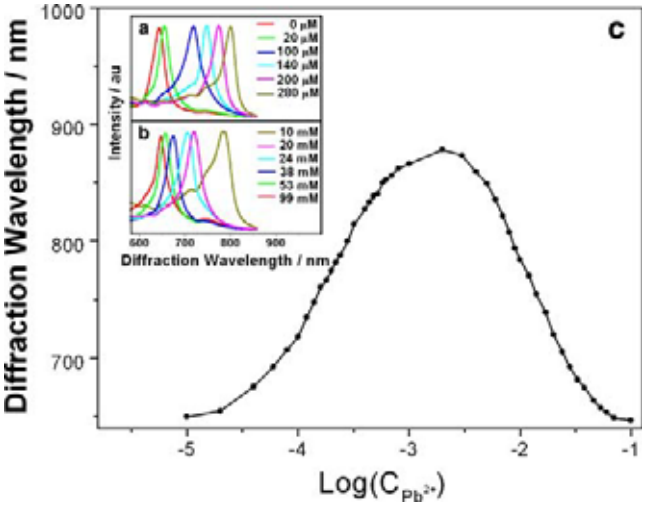

Fig. 1 **a** Response of PCCA to low Pb^{2+} concentrations. The diffraction wavelength redshifts. **b** Response of PCCA to high Pb^{2+} concentrations. The diffraction wavelength blueshifts. **c** Pb^{2+} concentration (log scale) dependence of PCCA diffraction wavelength. Lines connecting experimental data are included to guide the eye

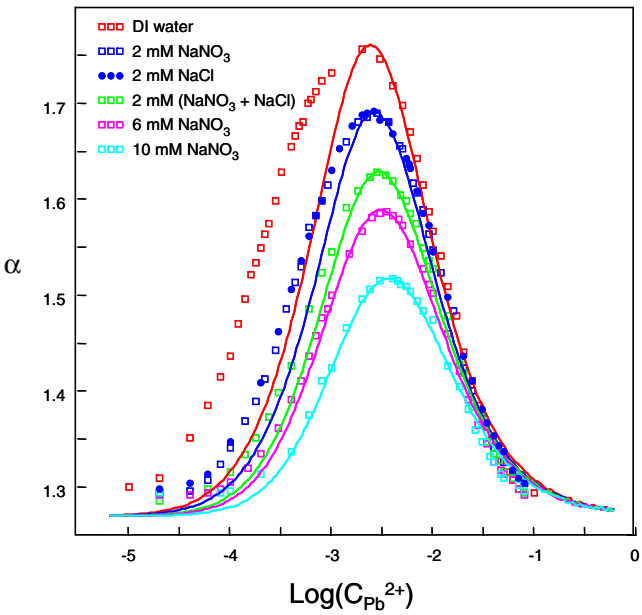

Fig. 2 Relative diffraction wavelength ratio ($\alpha=\lambda/\lambda_m$) of a PCCA as a function of $Pb(NO_3)_2$ concentration for various concentrations of $NaNO_3$ or NaCl. *Squares* and *circles* are experimental data. Lines are theoretical modeling results from the 1-D affine model

The response of the PCCA to Pb^{2+} results from the formation of an osmotic pressure in the hydrogel due to the immobilization of the Pb^{2+} by the PCCA crown ether [22, 28, 29]. This results in the formation of an ionic hydrogel in which the bound Pb^{2+} immobilizes its counterions and creates a Donnan equilibrium osmotic pressure for low Pb^{2+} concentrations [27]. This osmotic pressure swells the hydrogel and redshifts the diffraction, as shown in Fig. 1a. The Donnan potential is attenuated at high Pb^{2+} concentrations [26, 27], which decreases the hydrogel swelling and blueshifts the PCCA diffraction, as shown in Fig. 1b. Figure 1c shows the Pb^{2+} concentration dependence of the PCCA diffraction wavelength in pure water. The PCCA in pure water diffracts 642 nm light. As the Pb^{2+} concentration increases, the diffraction monotonically redshifts until the Pb^{2+} concentration is 2.3 mM. It then blueshifts with further increases in Pb^{2+} concentration; at a Pb^{2+} concentration of 99 mM, the diffraction blueshifts to 646 nm.

PCCA response to $Pb(NO_3)_2$ in sodium salt solutions (1-D swelling model) The ionic strength is defined by [50, 51]:

$$I = \frac{1}{2}\sum_i C_i z_i^2 \tag{17}$$

where C_i and z_i are the concentration and charge of the ith ion present in the solution, respectively. According to Eq. 17, for a monovalent salt solution, the ionic strength value is numerically equal to the concentration. Figure 2 shows the response of the PCCA to different Pb^{2+} concentrations for several monovalent sodium salt solutions. The experimental results are listed in Table 1. The response of the PCCA to Pb^{2+} in pure water is the largest, and decreases as the ionic strength increases. The Pb^{2+} concentration required to reach the maximal α increases with increasing salt concentrations.

We also observe that the response of the PCCA to Pb^{2+} is essentially identical in 2 mM $NaNO_3$ and 2 mM NaCl, which indicates that nonbinding monovalent anions impact equivalently on the reponse of the PCCA to Pb^{2+}. Based on Eqs. 16a and 16b, the volume equilibrium conditions defining the PCCA volume in solutions containing $Pb(NO_3)_2$ and NaX are:

$$\begin{aligned}
&[Na^+]_{in}[X^-]_{in} = [Na^+]_{out}[X^-]_{out}\\
&[Pb^{2+}]_{in}\left([NO_3^-]_{in}\right)^2 = [Pb^{2+}]_{out}\left([NO_3^-]_{out}\right)^2\\
&2[Pb^{2+}]_{in} + 2\left[(PCCA-PbL)^{2+}\right]\\
&\quad + [Na^+]_{in} - [X^-]_{in} - [NO_3^-]_{in} = 0
\end{aligned} \tag{18}$$

$$\Pi_{net} = \Pi_M + \Pi_{el} + \Pi_{ion} = 0$$

where X^- is the monovalent anion in the solution.

Table 1 Response of PCCA to Pb^{2+} in monovalent sodium salt solution. "Maximal α" is the maximal volume response of PCCA to Pb^{2+}, and "$C_{Pb}{}^{2+}$ (maximal α)" is the Pb^{2+} concentration required to reach the maximal α

	Maximal α	$C_{Pb}{}^{2+}$ (maximal α)
DI water	1.756	2.3 mM
2 mM $NaNO_3$	1.690	2.8 mM
2 mM NaCl	1.690	2.8 mM
2 mM ($NaNO_3$+NaCl)	1.630	2.9 mM
6 mM $NaNO_3$	1.587	3.5 mM
10 mM $NaNO_3$	1.518	4.0 mM

The expression for the Donnan osmotic pressure Π_{ion} is:

$$\frac{\Pi_{ion}}{RT} = \left[Pb^{2+}\right]_{in} + [Na^{+}]_{in} + \left[NO_3^{-}\right]_{in} + [X^{-}]_{in} - \left[Pb^{2+}\right]_{out} - [Na^{+}]_{out} - \left[NO_3^{-}\right]_{out} - [X^{-}]_{out} \quad (19)$$

Figure 2 also compares the experimental data to our theoretical model. For the response of PCCA to $Pb(NO_3)_2$ in pure water, we obtain good agreement between the model and experimental data for Pb^{2+} concentrations above 2.3 mM. However, we find systematic disagreement when modeling the response of the PCCA to $Pb(NO_3)_2$ for Pb^{2+} concentrations below 2.3 mM in pure water, as did Goponenko and Asher [27]. The observed response is much larger than that modeled. This response could be explained by an association constant in pure water which is approximately five-fold greater than that in solutions containing salts. We accurately model the response of the PCCA to $Pb(NO_3)_2$ in the presence of 10 mM $NaNO_3$.

PCCA response to $Pb(NO_3)_2$ in the presence of multivalent anions (1-D swelling model) The ionic strengths of solutions of 2 mM $NaNO_3$, 2 mM $Mg(NO_3)_2$ and 2 mM $Al(NO_3)_3$ are 2 mM, 6 mM and 12 mM, respectively. Figure 3a shows the PCCA response to $Pb(NO_3)_2$ in 2 mM $NaNO_3$. The maximal volume response is α=1.690, at a Pb^{2+} concentration of 2.8 mM. In contrast, in 2 mM $Mg(NO_3)_2$, the maximal volume response shows α=1.610, at a Pb^{2+} concentration of 3.4 mM. In 2 mM $Al(NO_3)_3$, the maximal volume response α=1.563, for a Pb^{2+} concentration of 3.3 mM. As the ionic strength increases, the volume response of PCCA to Pb^{2+} decreases. There also appears to be a small dependence on the Pb^{2+} concentration required to reach the maximal α.

Figure 3b compares the response to increasing Pb^{2+} concentrations at identical ionic strength of 2 mM $Mg(NO_3)_2$ solution and 6 mM $NaNO_3$ solutions. The responses to Pb^{2+} in these two salts are almost the same except for the region near the maximal volume response (the maximal α), where the maximal α value is 1.610 for 2 mM $Mg(NO_3)_2$ but only 1.587 for 6 mM $NaNO_3$. PCCA equilibrium conditions in $Mg(NO_3)_2$ along with those in $NaNO_3$ require:

1. The equality electrolyte activities inside and outside the PCCA [1]:

$$[Na^{+}]_{in}\left(\left[NO_3^{-}\right]_{in}\right) = [Na^{+}]_{out}\left(\left[NO_3^{-}\right]_{out}\right) \quad (20a)$$

$$\left[Mg^{2+}\right]_{in}\left(\left[NO_3^{-}\right]_{in}\right)^2 = \left[Mg^{2+}\right]_{out}\left(\left[NO_3^{-}\right]_{out}\right)^2 \quad (20b)$$

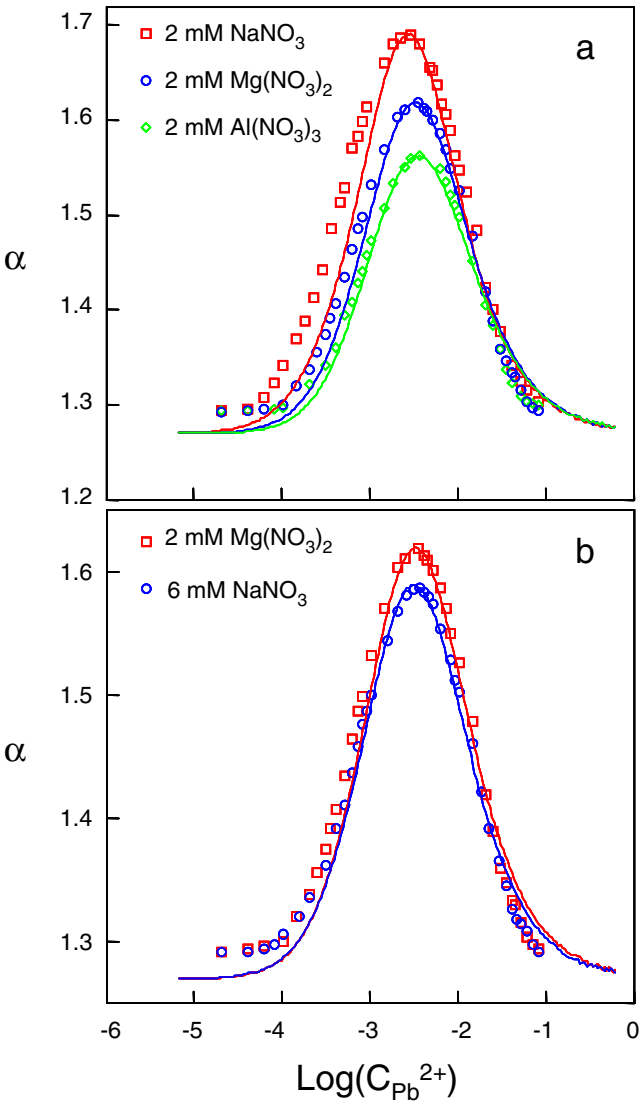

Fig. 3a, b Relative diffraction wavelength ratio ($\alpha = \lambda/\lambda_m$) of a PCCA as a function of $Pb(NO_3)_2$ concentration in (**a**) 2 mM of $NaNO_3$, $Mg(NO_3)_2$, or $Al(NO_3)_3$. **b** Comparison between 2 mM $Mg(NO_3)_2$ and 6 mM $NaNO_3$. *Squares*, *circles* and *diamonds* are experimental data. Lines show theoretical modeling results obtained using the 1-D affine model

where the exponent of $\left[NO_3^{-}\right]$ is 1 for $NaNO_3$ and 2 for $Mg(NO_3)_2$, due to their valences.

2. Electroneutrality is satisfied by [1]:

$$2\left[Pb^{2+}\right]_{in} + 2\left[(PCCA - PbL)^{2+}\right] + [Na^{+}]_{in} - \left[NO_3^{-}\right]_{in} = 0 \quad (21a)$$

$$2\left[Pb^{2+}\right]_{in} + 2\left[(PCCA - PbL)^{2+}\right] + 2\left[Mg^{2+}\right]_{in} - \left[NO_3^{-}\right]_{in} = 0 \quad (21b)$$

3. The Donnan osmotic pressure, Π_{ion}, in the $NaNO_3$ solution is:

$$\Pi_{ion} = RT\left(\left[Pb^{2+}\right]_{in} + \left[Na^{+}\right]_{in} + \left[NO_3^{-}\right]_{in} - \left[Pb^{2+}\right]_{out} - \left[Na^{+}\right]_{out} - \left[NO_3^{-}\right]_{out}\right) \quad (22a)$$

and in the $Mg(NO_3)_2$ solution is:

$$\Pi_{ion} = RT\left(\left[Pb^{2+}\right]_{in} + \left[Mg^{2+}\right]_{in} + \left[NO_3^{-}\right]_{in} - \left[Pb^{2+}\right]_{out} - \left[Mg^{2+}\right]_{out} - \left[NO_3^{-}\right]_{out}\right) \quad (22b)$$

Identical ionic strengths of $NaNO_3$ and $Mg(NO_3)_2$ occur at different concentrations of $NaNO_3$ and of $Mg(NO_3)_2$. The different equilibrium conditions result in a different response of the PCCA to Pb^{2+}, as shown in Fig. 3b.

Valence dependence of the response of the PCCA to Pb^{2+} (1-D swelling model) Identical ionic strength solutions of NaCl and $NaNO_3$ result in identical volume responses of the PCCA to Pb^{2+}. Identical ionic strength solutions of $Mg(NO_3)_2$ and $NaNO_3$ result in similar responses of the PCCA to Pb^{2+} except for the region near the maximal volume response, where the maximal volume response to $Mg(NO_3)_2$ is higher than that to $NaNO_3$.

In order to determine the effect of different cation valences on the response of the PCCA to Pb^{2+}, we modeled the responses of different AB_n solutions, where B^- is a monovalent anion. Since most multivalent anions (like CO_3^{2-}, SO_4^{2-} or PO_4^{3-}, etc.) precipitate Pb^{2+}, we only considered monovalent anions. The PCCA equilibrium in solutions of Pb^{2+} in the presence of dissolved and ionized AB_n is:

$$\left[A^{n+}\right]_{in}\left(\left[B^{-}\right]_{in}\right)^{n} = \left[A^{n+}\right]_{out}\left(\left[B^{-}\right]_{out}\right)^{n} \quad (23a)$$

$$\sum_{n} n\left[A^{n+}\right]_{in} + 2\left[Pb^{2+}\right]_{in} + 2\left[(PCCA - PbL)^{2+}\right] - \left[NO_3^{-}\right]_{in} - \left[B^{-}\right]_{in} = 0 \quad (23b)$$

and

$$\frac{\Pi_{ion}}{RT} = \sum_{n}\left(\left[A^{n+}\right]_{in} + \left[Pb^{2+}\right]_{in} + \left[B^{-}\right]_{in} + \left[NO_3^{-}\right]_{in} - \left[A^{n+}\right]_{out} - \left[Pb^{2+}\right]_{out} - \left[B^{-}\right]_{out} - \left[NO_3^{-}\right]_{out}\right) \quad (24)$$

The difference between Eqs. 16a, 16b and 23a, 23b is that Eqs. 16a, 16b are for an AB_n salt, while Eqs. 23a, 23b are for AB_n salt mixtures. We calculate the PCCA volume ratio V/V_m as a function of Pb^{2+} concentration in the four models by using Eqs. 23a, 23b and 24.

Figure 4 shows that in different AB_n solutions with identical ionic strengths, the volume response of the PCCA to Pb^{2+} is calculated to decrease in the order of AB_6, AB_5, AB_4, AB_3, AB_2 and AB. Thus, at identical ionic strengths the higher the valence of the cation A^{n+}, the larger the volume response of the PCCA to Pb^{2+}. Also, we observe that at high Pb^{2+} concentrations the responses are similar because the ionic strengths contributed by the AB_n salts are overwhelmed by that of $Pb(NO_3)_2$.

Figure 5 shows that the calculated response of the PCCA to Pb^{2+} for an AB_n solution is essentially identical to that of a mixture of AB_n, when the total solution ionic strengths are equal. We find that AB_n solutions with identical ionic strengths to solutions of a mixture of x AB_m salts show essentially the same response to Pb^{2+} if the following stoichiometry exists:

$$\frac{1}{x}\sum_{m}(A + m\ B) = A + n\ B \quad (25)$$

For example, for a mixture of AB_2, AB_3, AB_5, and AB_6 (each salt in the mixture has the same strength), based on Eq. 25

$$\frac{1}{4}(A + 2B + A + 3B + A + 5B + A + 6B) = A + 4\ B \quad (26)$$

However, we calculate different behaviors between pure salts and mixtures for cation valences ≥6, as shown in Fig. 6.

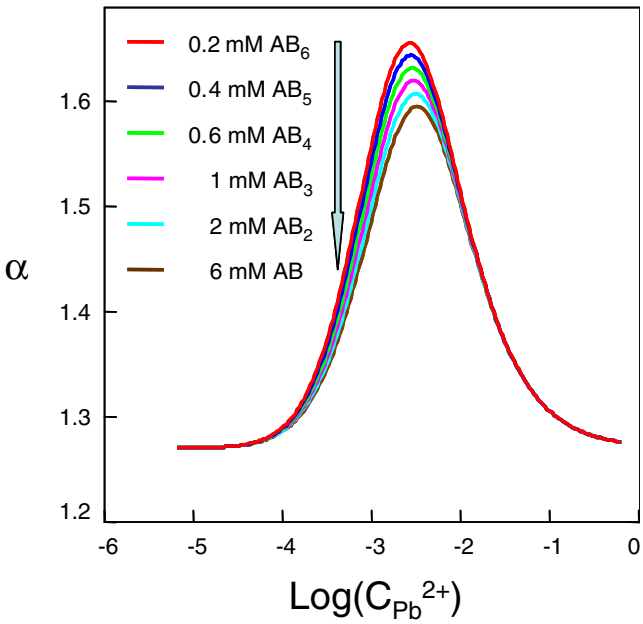

Fig. 4 Modeling of the responses of the PCCA to Pb^{2+} at identical ionic strength (6 mM) for 6 mM AB, 2 mM AB_2, 1 mM AB_3, 0.6 mM AB_4, 0.4 mM AB_5 and 0.29 mMAB_6 salts. All results are modeled using the 1-D affine model

Figure 7 shows that we calculate essentially identical responses to Pb^{2+} for solutions of AB_2 compared to solutions which are a mixture of AB and AB_3 at identical ionic strengths over a range of different ionic strength values.

PCCA response to $Pb(NO_3)_2$ during 3-D swelling All of the results above were for the PCCA attached to a substrate where the PCCA can only swell in the direction normal to the substrate plane. We also examined the the PCCA's response during 3-D swelling of a PCCA detached from the quartz plate. Figure 8a and b compare the PCCA's response to $Pb(NO_3)_2$ in pure water for 1-D swelling where the PCCA remains attached to the quartz plate to the free gel, which should be able to swell in all three dimensions. Removal of the gel from the plate causes the diffraction wavelength to decrease by ~12%, presumably because the hydrogel swells within the plane of the film causing the thickness to contract by ~12%.

Surprisingly the diffracted wavelength response (λ/λ_m) of the attached PCCA to Pb^{2+} is close to that of the free PCCA. Figure 8b shows the calculated volume response for

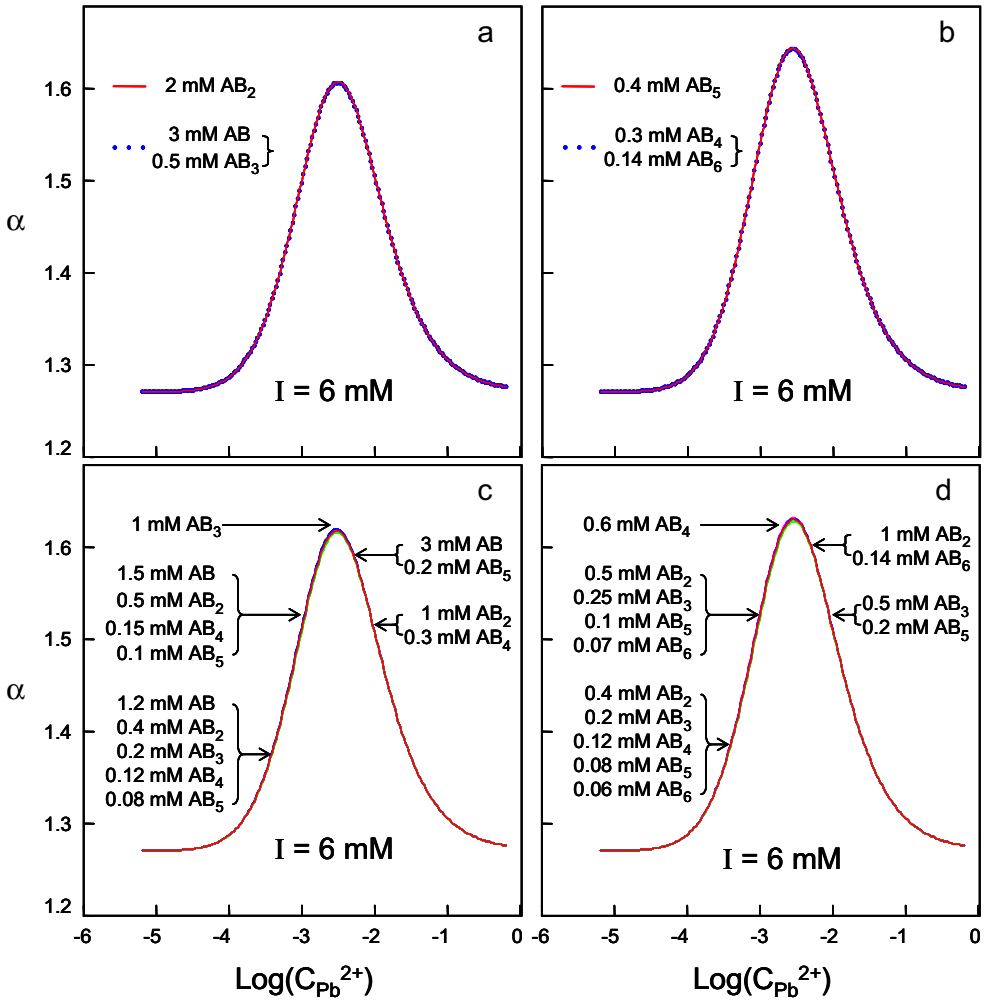

Fig. 5a–d Comparison between the responses of AB_n and mixture of AB_n salts at identical ionic strength. **a**: in 2 mM AB_2 and mixture of 3 mM AB and 0.5 mM AB_3; **b**: in 0.4 mM AB_5 and mixture of 0.3 mM AB_4 and 0.14 mM AB_6; **c**: in 1 mM AB_3, mixture of 3 mM AB and 0.2 mM AB_5, mixture of 1 mM AB_2 and 0.3 mM AB_4, mixture of 1.5 mM AB, 0.5 mM AB_2, 0.15 mM AB_4 and 0.1 mM AB_5, and mixture of 1.2 mM AB, 0.4 mM AB_2, 0.2 mM AB_3, 0.12 mM AB_4 and 0.08 mM AB_5; **d**: in 0.6 mM AB_4, mixture of 1 mM AB_2 and 0.14 mM AB_6, mixture of 0.5 mM AB_3 and 0.2 mM AB_5, mixture of 0.5 mM AB_2, 0.25 mM AB_3, 0.1 mM AB_5 and 0.07 mM AB_6, and mixture of 0.4 mM AB_2, 0.2 mM AB_3, 0.12 mM AB_4, 0.08 mM AB_5 and 0.06 mM AB_6. "*I*" is the ionic strength of AB_n or the mixture of AB_n salts. All results are modeled using the 1-D affine model

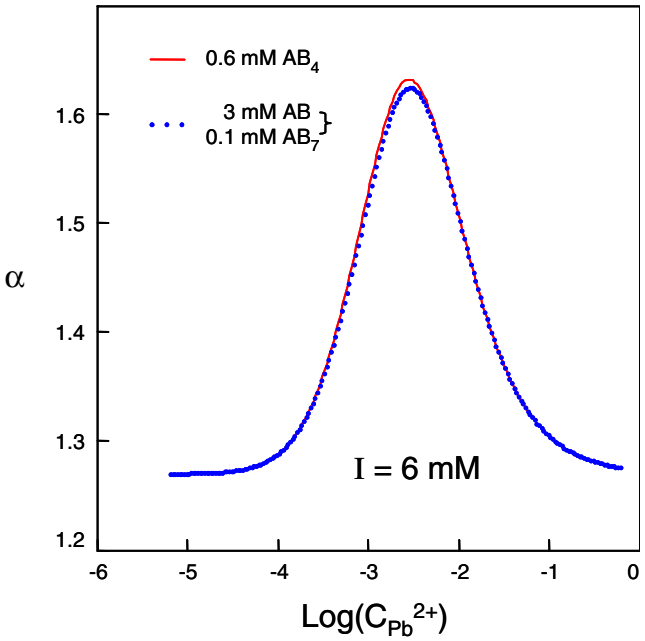

Fig. 6 Comparison between the responses of AB_4 and a mixture of AB and AB_7 at identical ionic strength. "*I*" is the ionic strength of AB_4 or the mixture of AB and AB_7. All results are modeled using the 1-D affine model

1-D and 3-D swelling. The much larger calculated response for 3-D swelling is not likely to be physically possible. It is possible that the original polymerization of the PCCA was inhomogeneous with extra crosslinking at the surfaces,

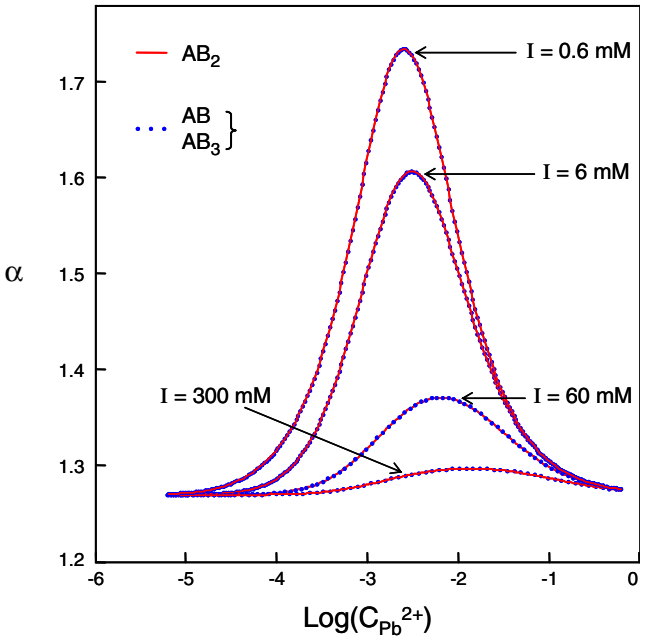

Fig. 7 Identical responses occur in a solution of AB_2 and in a mixture of AB and AB_3 for different ionic strengths, where the ionic strengths for AB_2 and the mixture are identical. "*I*" is the ionic strength of AB_2 or the mixture of AB and AB_3. All results are modeled using the 1-D affine model

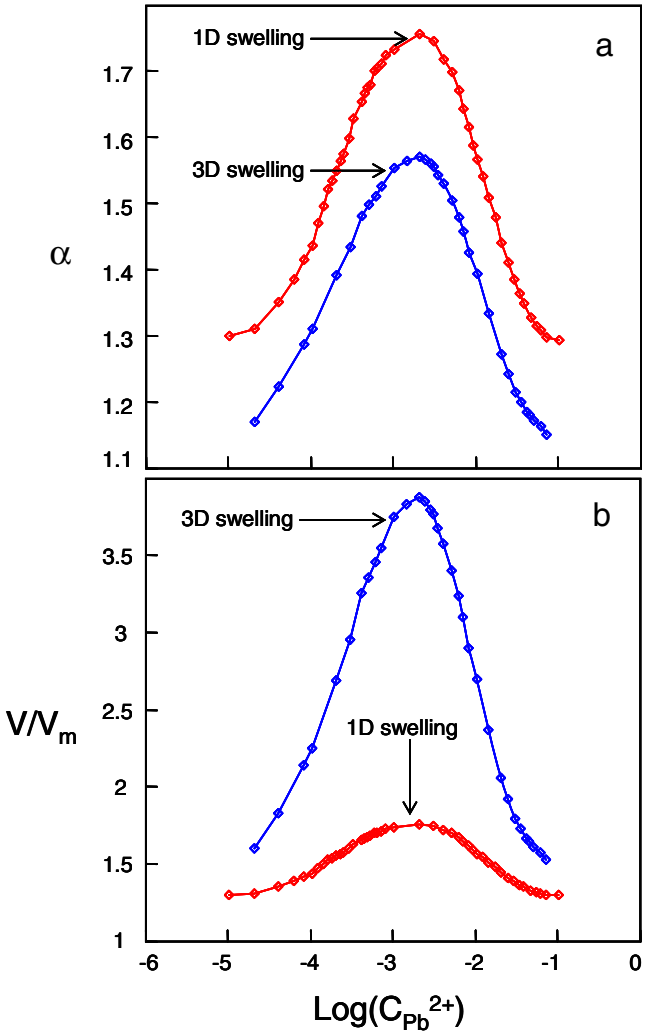

Fig. 8 **a** Measured relative diffraction wavelength ratio ($\alpha = \lambda/\lambda_m$) as a function of the $Pb(NO_3)_2$ concentration in pure water for 1-D swelling; **b** Calculated relative volume ratio (V/V_m) of a PCCA as a function of $Pb(NO_3)_2$ concentration in pure water for the 3-D swelling. Lines connecting data points are included to guide the eye

which maintains a 1-D swelling volume response. A similar result was observed by Goponenko et al., who explained the result through a remaining adhesion between the PCCA and the glass slide such that the free PCCA could swell in only one dimension [27].

Conclusions

We examined the response of a PCCA lead sensor to the addition of salts with different cation valences. By using a model based on Flory theory, we quantitatively modeled the response of the PCCA sensor to Pb^{2+} in pure water and to the presence of salts. We find that the response of the PCCA to Pb^{2+} in salt solutions depends on both the ionic strength and the valence of the counterion. With increasing ionic strength, the volume response of the PCCA to Pb

$(NO_3)_2$ decreases. Identical responses of the PCCA to Pb^{2+} occur for identical ionic strength solutions of NaCl and $NaNO_3$. However, different responses to Pb^{2+} occur between $Mg(NO_3)_2$ and $NaNO_3$ solutions for identical ionic strengths. The maximal volume response in $Mg(NO_3)_2$ is higher than that in $NaNO_3$. Comparing our model to the experimental data, we find we can accurately model the measured response of the PCCA to $Pb(NO_3)_2$ in solutions at high salt concentrations.

Acknowledgement We gratefully acknowledge financial support from NIH Grant EB004132. We are grateful to Dr Matti Ben-Moshe, who supplied us with his colloid.

References

1. Flory PJ (1953) Principles of polymer chemistry. Cornell University Press, Ithaca, NY
2. Dumitriu S (2002) Polymeric biomaterials, 2nd edn. Marcel Dekker, New York
3. Andrade JD (1976) Hydrogels for medical and related applications. American Chemical Society, Washington DC
4. DeRossi D, Kajiwara K, Osada Y, Yamauchi A (1991) Polymer gels: fundamentals and biomedical applications. Plenum, New York
5. Ottenbrite RM, Huang SJ, Park K (1996) Hydrogels and biodegradable polymers for bioapplications. American Chemical Society, Washington DC
6. Peppas NA (1987) Hydrogels in medicine and pharmacy. CRC Press, Boca Raton, FL
7. Peppas NA (1991) J Bioact Compat Polym 6:241
8. Park K, Shalaby SWS, Park H (1993) Biodegradable hydrogels for drug delivery. Technomic, Lancaster, PA
9. Weiss RG, Terech P (2006) Molecular gels: materials with self-assembled fibrillar networks. Springer, Berlin, Heidelberg, New York
10. Annaka M, Tanaka T (1992) Nature 355:430
11. Mafe S, Manzanares JA, English AE, Tanaka T (1997) Phys Rev Lett 79:3086
12. English AE, Tanaka T, Edelman ER (1997) J Chem Phys 107:1645
13. English AE, Tanaka T, Edelman ER (1998) Polymer 39:5893
14. Ricka J, Tanaka T (1984) Macromolecules 17:2916
15. Hirokawa Y, Tanaka T, Sato E (1985) Macromolecules 18:2782
16. Kudaibergenov SE, Sigitov VB (1999) Langmuir 15:4230
17. Kim JJ, Park K (1999) Bioseparation 7:177
18. Hassan CM, Doyle FJ III, Peppas NA (1997) Macromolecules 30:6166
19. Park K (1997) Controlled drug delivery. American Chemical Society, Washington DC
20. Lee KY, Moony DJ (2001) Chem Rev 101:1869
21. Miyata T, Uragami T, Nakamae K (2002) Adv Drug Delivery Rev 54:79
22. Holtz JH, Asher SA (1997) Nature 389:829
23. Holtz JH, Janet SWH, Munro CH, Asher SA (1998) Anal Chem 70:780
24. Asher SA, Peteu SF, Reese CE, Lin MX, Finegold DN (2002) Anal Bioanal Chem 373:632
25. Walker JP, Asher SA (2005) Anal Chem 77:1596
26. Reese CE, Asher SA (2003) Anal Chem 75:391
27. Goponenko AV, Asher SA (2005) J Am Chem Soc 127:10753
28. Reese CE, Baltusavich ME, Keim JP, Asher SA (2001) Anal Chem 73:5038
29. Asher SA, Sharma AC, Goponenko AV, Ward MM (2003) Anal Chem 75:1676
30. Lee K, Asher SA (2000) J Am Chem Soc 122:9534
31. Alexeev VL, Sharma AC Goponenko AV, Das S, Lednev IK, Wilcox CS, Finegold DN, Asher SA (2003) Anal Chem 75:2316
32. Asher SA, Alexeev VL, Goponenko AV, Sharma AC, Lednev IK, Wilcox CS, Finegold DN (2003) J Am Chem Soc 125:3322
33. Reese CE, Guerrero CD, Weissman JM, Lee K, Asher SA (2000) J Colloid Interf Sci 232:76
34. Mark JE, Erman B (1988) Rubberlike elasticity, a molecular primer. Wiley, New York
35. James HM, Guth E (1942) Ind Eng Chem 34:1365
36. James HM (1947) J Chem Phys 15:651
37. James HM, Guth E (1947) J Chem Phys 15:669
38. Flory PJ (1950) J Chem Phys 18:108
39. Wall FT, Flory PJ (1951) J Chem Phys 19:1435
40. Asher SA, Flaugh PL, Washinger G (1986) Spectroscopy 1:26
41. Carlson RJ, Asher SA (1984) Appl Spectrosc 38:297
42. Asher SA, Holtz JH, Liu L, Wu Z (1994) J Am Chem Soc 116:4997
43. Weissamn JM, Sunkara HB, Tse AS, Asher SA (1996) Science 274:959
44. Pan G, Sood AK, Asher SA (1988) J Appl Phys 84:83
45. Okubo T (1988) Acc Chem Res 21:281
46. Izatt RM, Terry RE, Nelson DP, Chan Y, Eatough DJ, Bradshaw JS, Hansen LD, Christensen JJ (1976) J Am Chem Soc 98:7626
47. Izatt RM, Terry RE, Haymore BL, Hansen LD, Dalley NK, Ayondet AG, Christensen JJ (1976) J Am Chem Soc 98:7620
48. Manege LC, Takayanagi T, Oshima M, Iwachido T, Motomizu S (1999) Bull Chem Soc Jpn 72:1301
49. Goldcamp MJ, Ashley K, Edison SE, Pretty J, Shumaker J (2005) Electroanalysis 17:1015
50. Lewis GN, Randall M (1921) J Am Chem Soc 43:1112
51. Pitzer KS (1984) J Chem Educ 61:104